A Gravitational Model for Grayscale Texture Classification Applied to the *pap-smear* Database

Jarbas Joaci de Mesquita Sá Junior[1] and André R. Backes[2](✉)

[1] Departamento de Engenharia de Computação, Campus de Sobral - Universidade Federal do Ceará, Rua Estanislau Frota, S/N, Centro, Sobral, Ceará CEP: 62010-560, Brazil
jarbas_joaci@yahoo.com.br

[2] Faculdade de Computação, Universidade Federal de Uberlândia, Av. João Naves de Ávila, 2121, Uberlândia, MG CEP: 38408-100, Brazil
arbackes@yahoo.com.br

Abstract. This paper presents the application of a novel and very discriminative texture analysis method based on a gravitational model to a relevant medical problem, which is to classify *pap-smear* cell images. For this purpose, the complexity descriptors Bouligand-Minkowski fractal dimension and lacunarity were employed to extract signatures from the gravitational collapsing process. The obtained result was compared to other texture analysis methods. Additionally, AUC measure performance was computed and compared to several LBP based descriptors presented in two recent papers. The performed comparisons demonstrate that texture analysis based on gravitational model is suitable for discriminating *pap-smear* images.

Keywords: *pap-smear* database · Gravitational model · Bouligand-Minkowski fractal dimension · Lacunarity

1 Introduction

Computer vision has been successfully applied to many medical problems, such as discriminating normal and abnormal tissues, segmenting a region of interest (e.g., a tumor image), associating a determined image pattern to a disease etc. These applications contribute significantly to medical diagnosis, sometimes reinforcing the specialist's opinion or providing information that cannot be perceived by the human eye. One can cite as instances from the large set of works of computer vision applied to medical purposes: paper [1] classifies breast tissues into normal and abnormal tissues, and these abnormal tissues into benign and malignant cancer; paper [2] uses texture measures for meningioma classification of histopathological images; and paper [3] classifies dermoscopy images to differentiate between melanomas and benign melanocytic lesions.

V. Murino and E. Puppo (Eds.): ICIAP 2015, Part II, LNCS 9280, pp. 332–339, 2015.
DOI: 10.1007/978-3-319-23234-8_31

Among the several attributes that can be analyzed in a medical image, such as color and shape, texture is surely one of the most important. Texture concept can be understood as the distribution and spatial dependency among pixels in a determined local area [4]. This description, however, is more suitable for artificial textures. Natural textures (e.g., images of smoke, leaf, wood) present persistent quasi-periodic patterns, resulting in a cloud-like appearance [5]. There is a great variety of methods for texture analysis, ranging from classical approaches, such as co-occurrence matrices [4] and wavelet descriptors [6], to state-of-the-art methods, such as tourist walk [7] and shortest paths in graphs [8].

This work aims to apply a texture analysis method based on a simplified gravitational system to grayscale images from the *pap-smear* dataset. This dataset is composed by human cell images obtained from the cervix [9]. This is an extension of the works previously published in [10,11]. Here we focus on the application of the technique in a new variety of digital images and not in the development or refinement of the method. This is a way of measuring the applicability of our method in biological problems, thus aiming to contribute to the diagnosis of diseases.

The paper is organized as follows: Section 2 briefly describes the gravitational system for images. Section 3 presents the procedure to obtain an image signature based on two complexity descriptors (Bouligand-Minkowski fractal dimension and lacunarity), which are extracted from the gravitational collapse process. Section 4 describes the experiments performed on the grayscale *pap-smear* database. Section 5 shows the superior performance of the presented method in comparison to other important texture analysis methods. Finally, Section 6 establishes some considerations of this work.

2 Gravitational Model

The gravitational model applied in this work aims to extract additional information from images in order to construct more discriminative feature vectors. For this purpose, each pixel is interpreted as a particle whose mass is its own intensity. Next, a central mass M located at the image center is used to attract each pixel towards itself. This mass M is calculated for each image according to the mean of its dimensions. This is performed because images from the *pap-smear* database are rectangular. Moreover, there is no interaction among the pixels, only between each pixel and the central mass. Also because *pap-smear* images are rectangular, no tangential velocity is established to the image pixels. Thus, all the pixels have an acceleration $\boldsymbol{a}_{pix}$ toward the image center according to the following equation

$$\boldsymbol{a}_{pix} = \begin{cases} G.M/\left\|\boldsymbol{r}\right\|^2 & \text{if} \quad I(x,y) \neq 0 \\ 0, & \text{if} \quad I(x,y) = 0, \end{cases} \tag{1}$$

where G is the gravitational constant, r is the distance vector between the pixel and the image center, and $I(x,y)$ is the pixel intensity. The distance covered by the pixel is $S = (1/2).\left\|\boldsymbol{a}_{pix}\right\|.t^2$, where t is the time step.

Adopting this procedure it is possible to simulate a collapsing gravitational process from the original image. Each image that represents a stage of this collapsing process (i.e., the collapsing process in a determined time step t) can be explored by complexity descriptors, such as Bouligand-Minkowski fractal dimension and lacunarity. A detailed description of the gravitational approach can be found in the papers [10,11].

3 Signature for Grayscale Textures

Different images produce different gravitational systems, and each one will collapse in its own way. So, it is interesting to measure each collapsing state in order to achieve a multiscale signature for the original image. In previous studies [10,11], we proposed to represent a collapsing image computed at time t using fractal dimension and lacunarity values. Fractal dimension is a widely used tool to describe objects (shape and texture) in terms of theirs irregularity and space occupation [12,13]. For this task we used the Bouligand-Minkowski fractal dimension. This method uses a function $\mathrm{f} : I(x, y) \rightarrow S(x, y, I(x, y))$ to create a surface $S \in R^3$ from a texture pattern I. Then, it computes the influence volume $V(r)$ of this surface by dilating each point of S with a sphere of radius r:

$$V(r) = \left|\left\{s' \in R^3 | \exists s \in S : |s - s'| \leq r\right\}\right|. \tag{2}$$

The Bouligand-Minkowski fractal dimension D is estimated as

$$D = 3 - \lim_{r \to 0} \frac{\log V(r)}{\log r}. \tag{3}$$

There are cases where different texture patterns present the same fractal dimension, thus making this method inefficient. To solve this problem Mandelbrot introduced the lacunarity: a method that describes a texture pattern in terms of spatial dispersion using a specific gap size [12,14]. For this study, we use the gliding-box algorithm to compute the lacunarity [14,15]. Basically, this algorithm uses a box of $l \times l$ pixels size to compute the distribution of gaps in the image. As this box glides over the image, the algorithm calculates the relative height for that portion of the image

$$h_l(i, j) = \lceil v/l \rceil - \lceil u/l \rceil, \tag{4}$$

where u and v are the minimum and maximum pixel values inside the box, respectively. From the probability density function $Q_l(H)$ of the relative height $h_l(i, j)$, the lacunarity for a box size l is defined as

$$\Lambda(l) = \sum H^2.Q_l(H) / \left(\sum H.Q_l(H)\right)^2. \tag{5}$$

Since we are able to compute more than one collapsing stage per image, we propose a feature vector which is the concatenation of these values computed for a set of time steps $T = \{t_1, t_2, \ldots, t_k\}$, as described as follows:

$$\psi_{T,R,L} = [D_{t_1}(R), \ldots, D_{t_k}(R), \Lambda_{t_1}(L), \ldots, \Lambda_{t_k}(L)] , \qquad (6)$$

where $D_t(R)$ and $\Lambda_t(L)$ represent, respectively, the set of fractal and lacunarity descriptors computed for a specific set of radii and box sizes, $R = \{r_1, r_2, \ldots, r_N\}$ and $L = \{l_1, l_2, \ldots, l_M\}$.

By using both fractal dimension and lacunarity we improve the discrimination of the collapsing process. This is due to the great sensitiveness to measure structural changes from the fractal dimension combined to the ability of the lacunarity to discriminate systems that are similar in terms of fractal dimension although different in their structures.

4 Experiments

4.1 *pap-smear* Database

The *pap-smear* [9] database is composed by 917 images extracted from the cervix. This images are divided into the following cell types: normal superficial squamous epithelial (74 images); normal intermediate squamous epithelial (70 images); normal columnar epithelial (98 images); mild squamous non-keratinizing dysplasia (182 images); abnormal moderate squamous non-keratinizing dysplasia (146 images); abnormal severe squamous non-keratinizing dysplasia (197 images); and abnormal squamous cell carcinoma in situ intermediate (150 images). Two categories can be used to classify these images: normal (242 images) and abnormal (675 images). Figure 1 shows a sample from each cell type as well as their classifications. In the experiments, we considered only these two classes, as the 7-classes problem is still difficult to deal with texture analysis methods. Moreover, we converted all the images into grayscale by considering only its luminance.

4.2 Methods and Classification

To perform a more accurate evaluation of our approach, we compared the gravitational model to other important texture analysis methods using the highest obtained accuracy as criterion. The compared methods are:

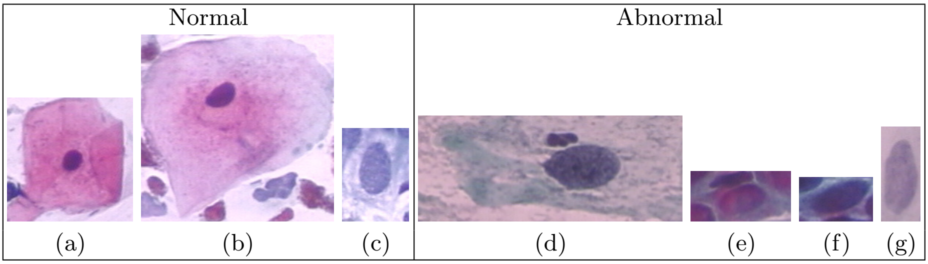

Fig. 1. Samples of the *pap-smear* database: a - superficial squamous epithelial, b - intermediate squamous epithelial, c - columnar epithelial, d - mild squamous non-keratinizing dysplasia, e - moderate squamous non-keratinizing dysplasia, f - severe squamous non-keratinizing dysplasia, g - squamous cell carcinoma in situ intermediate.

Tourist walk [7]: this method interprets each pixel as a tourist that visits cities (i.e., other pixels) adopting as criterion to choose the closest (or farthest) city not visited in the last μ (tourist memory parameter) time steps. In the experiments, we used the time steps $\mu = \{0, 1, 2, 3, 4, 5\}$ for the minimum and maximum distance. This resulted in a feature vector of 48 attributes for each tourist histogram.

Wavelet descriptors [6,16]: a multilevel 2D wavelet decomposition is performed with three dyadic decompositions using daubechies 4. Energy and entropy were computed from horizontal, vertical and diagonal details, resulting in a feature vector of 18 attributes.

Co-occurrence matrices [4]: this method quantifies the co-occurrence of a pair of pixels i and j in a determined direction θ and distance d. In the experiments, we used the directions $\theta = \{0^\circ, 45^\circ, 90^\circ, 135^\circ\}$ and distances $d = \{1, 2\}$. We also used non-symmetric matrices. For each matrix, we computed energy and entropy descriptors. This resulted in an image signature of 16 features.

For the classification of the samples, we used Linear Discriminant Analysis (LDA) [17]. This supervised statistical method aims to maximize the inter-class variance and minimize the intra-class variance. In the experiments with this classifier, the leave-one-out cross validation scheme was employed. This strategy consists of using one sample for validation and the remainder $N - 1$ samples for training, where N is the total of samples. This process is repeated N times, each time with a different sample for testing.

Additionally, we performed a comparison against two recent papers [18,19] using Area Under the ROC Curve (AUC) [20] as performance measurement. The paper [18] applies a total of nine LBP variants to the *pap-smear* database, and the paper [19] presents a large list of LBP based descriptors applied to this same database (more than 50 different tests were performed). These two papers use a Linear Support Vector Machine (SVM) for classification and the strategy 5-fold cross-validation. This validation scheme consists of dividing the dataset into five subsets, one subset used for testing and the remainder four subsets for training. This process is repeated five times, each time with a different subset for testing. The paper [18] does not describe which parameters C and γ were used in SVM, but the paper [19] uses the default values of C and γ of LIBSVM, a public library for SVM [21]. The experiments performed in this work use these same default parameter values. The highest AUC of each paper was compared to the gravitational model performance.

5 Results

Before applying the gravitational approach, we set the gravitational constant G to 1, according to the paper [10]. Next, we tested different sets of radii $R = \{3, 4, \ldots, 8\}$ and window sizes $L = \{2, 3, \ldots, 19\}$, for the same set of time steps $T = \{1, 3, 6, 9\}$ in order to find the combination that yields the highest accuracy, as can be seen in Table 1. We chose to use non-sequential time steps as they minimize the amount of redundant information that two sequential values of t

Table 1. Accuracy (%) of the gravitational model method on the *pap-smear* database for sets $R = \{3, \ldots, r_{max}\}$ and $L = \{2, \ldots, l_{max}\}$ values and the same time set $T = \{1, 3, 6, 9\}$

	r_{max}			
l_{max}	5	6	7	8
10	85.71	85.82	85.49	85.82
12	86.80	86.25	86.15	86.36
14	87.13	87.24	87.35	87.56
16	86.80	87.35	87.89	87.56
18	88.11	88.11	87.89	88.44
20	87.02	87.45	87.78	87.89

may share, thus improving the discrimination ability of the method. We also noticed that there is a small but consistent increase in the success rate as we increase the number of fractal and lacunarity descriptors used. We obtained the highest accuracy with the following parameter values: $R = \{3, 4, \ldots, 8\}$ and $L = \{2, 3, \ldots, 18\}$.

Table 2 shows the comparison of the gravitational model with other grayscale texture analysis methods using accuracy as measurement performance. The gravitational approach surpassed all the other methods. Moreover, the obtained accuracy is 2.07% superior to the second best method (wavelet descriptors). This represents an amount of more 19 images corrected classified. This corroborates the efficiency and the discrimination power of the presented method, as the *pap-smear* database is hard to classify and any improvement is desirable.

Table 2. Comparison results of different methods applied to the *pap-smear* database

Methods	No of descriptors	Accuracy (%)
Gravitational model	92	88.44
Wavelet descriptors	18	86.37
Tourist walk	48	85.82
Co-occurrence matrices	16	79.83

The comparison with LBP based descriptors confirms the high performance of the gravitational model, as can be seen in Table 3. The results of the presented method surpassed all the results presented in the [18]. Moreover, it yields AUC value superior to more than 90% of the LBP based descriptors presented in the paper [19].

Table 3. Comparison of the gravitational model with LBP based descriptors applied to the *pap-smear* database

Methods	AUC
Gravitational model	0.8915
ENS (Highest AUC in the paper [18])	0.8840
MAG1 (Highest AUC in the paper [19])	0.9080

6 Conclusion

This work presented an application of a powerful texture analysis method to a challenging medical database, which consists of *pap-smear* images. The obtained accuracy and AUC values were superior to almost all the compared methods, demonstrating that the gravitational approach is suitable for this specific set of medical images. The results indicated that future improvements in the gravitational model will lead to still better classification rates in the *pap-smear* database.

Acknowledgments. André R. Backes gratefully acknowledges the financial support of CNPq (National Council for Scientific and Technological Development, Brazil) (Grant #301558/2012-4), FAPEMIG and PROPP-UFU. Jarbas Joaci de Mesquita Sá Junior gratefully acknowledges the financial support of CNPq (National Council for Scientific and Technological Development, Brazil) (Grant #453298/2015-0).

References

1. Braz Junior, G., Paiva, A.C., Silva, A.C., Oliveira, A.C.M.: Classification of breast tissues using Moran's index and Geary's coefficient as texture signatures and SVM. Computers in Biology and Medicine **39**(12), 1063–1072 (2009)
2. Al-Kadi, O.S.: Texture measures combination for improved meningioma classification of histopathological images. Pattern Recognition **43**(6), 2043–2053 (2010)
3. Abbas, Q., Celebi, M., Serrano, C., García, I.F., Ma, G.: Pattern classification of dermoscopy images: A perceptually uniform model. Pattern Recognition **46**(1), 86–97 (2013)
4. Haralick, R.M.: Statistical and structural approaches to texture. Proceedings of the IEEE **67**(5), 786–804 (1979)
5. Kaplan, L.M.: Extended fractal analysis for texture classification and segmentation. IEEE Transactions on Image Processing **8**(11), 1572–1585 (1999)
6. Chang, T., Kuo, C.J.: Texture analysis and classification with tree-structured wavelet transform. IEEE Transactions on Image Processing **2**(4), 429–441 (1993)
7. Backes, A.R., Gonçalves, W.N., Martinez, A.S., Bruno, O.M.: Texture analysis and classification using deterministic tourist walk. Pattern Recognition **43**(3), 685–694 (2010)
8. Sá Junior, J.J.M., Backes, A.R., Cortez, P.C.: Texture analysis and classification using shortest paths in graphs. Pattern Recognition Letters **34**(11), 1314–1319 (2013)
9. Jantzen, J., Norup, J., Dounias, G., Bjerregaard, B.: Pap-smear benchmark data for pattern classification. In: Proc. NiSIS 2005, Albufeira, Portugal, NiSIS, pp. 1–9 (2005)
10. Sá Junior, J.J.M., Backes, A.R.: A simplified gravitational model to analyze texture roughness. Pattern Recognition **45**(2), 732–741 (2012)
11. Sá Junior, J.J.M., Backes, A.R., Cortez, P.C.: A simplified gravitational model for texture analysis. Journal of Mathematical Imaging and Vision **47**(1–2), 70–78 (2013)
12. Mandelbrot, B.: The fractal geometry of nature. Freeman & Co. (2000)

13. Backes, A.R., Casanova, D., Bruno, O.M.: Color texture analysis based on fractal descriptors. Pattern Recognition **45**(5), 1984–1992 (2012)
14. Allain, C., Cloitre, M.: Characterizing the lacunarity of random and deterministic fractal sets. Phys. Rev. A **44**(6), 3552–3558 (1991)
15. Du, G., Yeo, T.S.: A novel lacunarity estimation method applied to SAR image segmentation. IEEE Trans. Geoscience and Remote Sensing **40**(12), 2687–2691 (2002)
16. Daubechies, I.: Ten lectures on wavelets. Society for Industrial and Applied Mathematics, Philadelphia (1992)
17. Everitt, B.S., Dunn, G.: Applied Multivariate Analysis, 2nd edn. Arnold (2001)
18. Nanni, L., Lumini, A., Brahnam, S.: Local binary patterns variants as texture descriptors for medical image analysis. Artificial Intelligence in Medicine **49**(2), 117–125 (2010)
19. Nanni, L., Lumini, A., Brahnam, S.: Survey on LBP based texture descriptors for image classification. Expert Systems with Applications **39**(3), 3634–3641 (2012)
20. Fawcett, T.: An introduction to ROC analysis. Pattern Recognition Letters **27**(8), 861–874 (2006)
21. Chang, C.C., Lin, C.J.: LIBSVM: A library for support vector machines. ACM Transactions on Intelligent Systems and Technology **2**, 27:1–27:27 (2011)